Primary mirror figure maintenance of the Hobby-Eberly Telescope using the segment alignment maintenance system

Rakoczy, John, Hall, Drew, Howard, Richard, Ly, William, Weir, John, et al.

John M. Rakoczy, Drew Hall, Richard T. Howard, William Ly, John T. Weir, Edward E. Montgomery IV, Mark T. Adams, John A. Booth, James R. Fowler, Gregory H. Ames, "Primary mirror figure maintenance of the Hobby-Eberly Telescope using the segment alignment maintenance system," Proc. SPIE 4837, Large Ground-based Telescopes, (4 February 2003); doi: 10.1117/12.456734

SPIE.

Event: Astronomical Telescopes and Instrumentation, 2002, Waikoloa, Hawai'i, United States

Primary mirror figure maintenance of the Hobby-Eberly Telescope using the Segment Alignment Maintenance System

John Rakoczy[a], Drew Hall[a], Ricky Howard[a], William Ly[a], John Weir[a], Edward Montgomery[a], Mark Adams[b], John Booth[b], James Fowler[b], Greg Ames[c]
[a]NASA Marshall Space Flight Center; [b]The University of Texas at Austin; [c]Blue Line Engineering

ABSTRACT

The Segment Alignment Maintenance System (SAMS) was installed on McDonald Observatory's Hobby-Eberly Telescope (HET) in August 2001. The SAMS became fully operational in October 2001. The SAMS uses a system of 480 inductive edge sensors to correct misalignments of the HET's 91 primary mirror segments when the segments are perturbed from their aligned reference positions. A special observer estimates and corrects for the global radius of curvature (GRoC) mode, a mode unobservable by the edge sensors. The SAMS edge sensor system and GRoC estimator are able to maintain HET's primary figure for longer durations than previously had been observed. This paper gives a functional description of the SAMS control system and presents performance verification data.

Keywords: segmented mirror, edge sensors, control system, Hobby-Eberly Telescope

INTRODUCTION

The Hobby-Eberly Telescope (HET) is a 9.2-m fixed elevation telescope with a segmented primary mirror (91 segments). It is located at McDonald Observatory in West Texas at an elevation of 2,008m. During initial testing of the telescope after first light, composite star image spots formed by individual mirror segments were observed to "de-stack", or move with respect to each other, over a period of time after the segments had been "stacked", or aligned with each other. While minor segment motion over a period of an hour or more had been anticipated in the original design, misalignment of the segments on a time scale of tens of minutes under some conditions was unexpected. In November 1999, the University of Texas at Austin entered into a Space Act Agreement with NASA's Marshall Space Flight Center (MSFC) to procure a Segment Alignment Maintenance System (SAMS) for the HET[1]. The objective of the SAMS is to correct the effects of the de-stacking phenomenon, thereby maintaining primary mirror segment alignment. MSFC teamed with Blue Line Engineering of Colorado Springs, Colorado. Blue Line provided the edge sensing system and electronics. MSFC developed control algorithms and control system software. MSFC also managed system integration and verification testing.

The SAMS consists of 480 inductive edge sensors, up to 6 sensors per mirror segment. Each sensor head assembly weighs less than 50 grams. Each segment has its own local electronics or "hub." The 91 segments are subdivided into 3 groups or "nodes" comprising 30 or 31 segments each. Each node feeds into its respective cluster control processor (CCP). A master system control processor (SCP), which resides with the CCPs in the Stackable System Processor (SSP), coordinates the three CCPs and transmits all 480 channels of edge sensor measurements to the SAMS control computer, a Sun Sparc Ultra 5 workstation, once every second. On the SAMS control computer, LabVIEW-based software acquires the edge sensor measurements, checks for health, corrects errors, archives data, computes mirror motion correction commands and sends the commands to the HET's primary mirror computer (PMC). The PMC typically queries the SAMS computer for corrections every 90 seconds. Detailed descriptions of the SAMS hardware, software, architecture and interfaces can be found elsewhere in the literature[1,2,4].

Large Ground-based Telescopes, Jacobus M. Oschmann, Larry M. Stepp, Editors,
Proceedings of SPIE Vol. 4837 (2003) © 2003 SPIE · 0277-786X/03/$15.00

The emphasis of this paper is to describe how the edge sensors were used in a control system strategy to maintain the HET's primary mirror figure. Maintaining the primary mirror figure involved implementing a controller that would globally minimize the edge-matching shear errors across segment gaps while maintaining the correct radius-of-curvature of the primary mirror. This paper describes the derivation of the optimal controller and the architecture under which it was implemented in the SAMS LabVIEW-based software. This paper also describes the phenomena driving the global radius-of-curvature (GRoC) mode and the approaches to controlling the GRoC mode. HET performance characterization data are presented, highlighting the success of SAMS in controlling low-frequency dynamics disturbances while illuminating SAMS's inherent limitations when subject to temperature changes.

1. DERIVATION OF OPTIMAL CONTROL

This section briefly describes the derivation of the optimal control system gains implemented in the SAMS software. A detailed derivation of the influence matrix and optimal control can be found in the references[8]. The derivation starts with the influence function relating all the segment degrees of freedom to the edge sensor outputs. The general influence function relating all tip, tilt and piston degrees of freedom to edge sensor outputs is the following:

$$e = C_{480x273} x_{273x1} \tag{1.1}$$

The vector e comprises all 480 edge sensor measurements. The vector x comprises all 273 tip, tilt and piston degrees of freedom of the primary mirror. The matrix $C_{480x273}$ is the full-array influence matrix. It is the goal of the optimal controller to minimize, in a least squares manner, the following cost function:

$$J = (e_{ref} - e)^T (e_{ref} - e) \tag{1.2}$$

The vector e_{ref} constitutes the edge sensor measurements taken when the mirror was aligned to the position yielding the best possible image quality. Those edge sensor measurements are the control system set points. The control which minimizes J is the following:

$$u = (C_{480x273}^T C_{480x273})^{-1} C_{480x273}^T (e_{ref} - e) \tag{1.3}$$

In equation 1.3, the vector u has dimension 273x1, comprising all degrees of freedom. However, the influence matrix $C_{480x273}$ only has rank 269 with the global tip, tilt, piston and radius-of-curvature modes in its null space. Therefore, equation 1.3 does not yield a unique least-squares optimal controller (besides the fact that $C_{480x273}^T C_{480x273}$ is not invertible). In order to fully constrain the optimization problem, four boundary conditions were introduced. Four segments' piston degrees of freedom were constrained mathematically in order to establish the boundary conditions. When the four boundary condition constraints are imposed, one obtains a diminished influence matrix $C_{480x269}$. The four piston boundary conditions are on the shaded segments shown in Figure 1 (M43, M25, M28 and M74). The optimal control system gains are computed from the modified influence matrix according to the following equation:

$$K = (C_{480x269}^T C_{480x269})^{-1} C_{480x269}^T \tag{1.4}$$

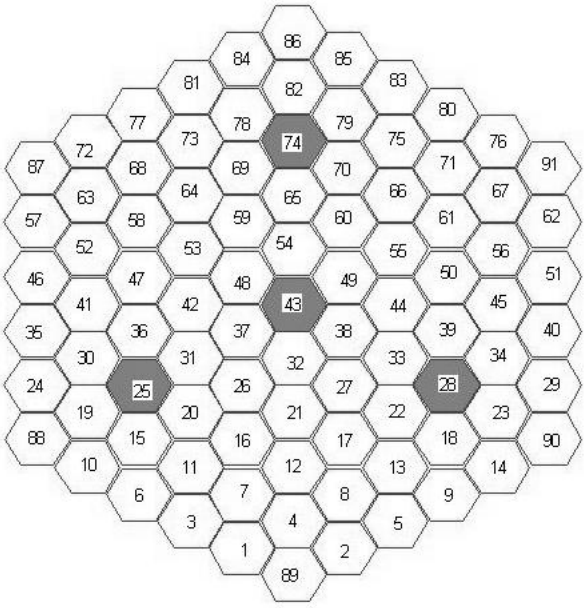

Figure 1: HET segment layout with SAMS boundary conditions

Thus, control gain matrix K is the pseudoinverse of the modified influence matrix $C_{480x269}$. $C_{480x269}$ is full rank, so $(C_{480x269}{}^{T}C_{480x269})$ is invertible. The dimension of K is 269x480. Then the control command to the 269 active degrees of freedom is the following:

$$u_{269x1} = K(e_{ref} - e) \tag{1.5}$$

A consequence of the imposition of the boundary conditions is that 4 primary mirror modes remain uncontrolled. For the Hobby-Eberly Telescope, global tip, tilt and piston are of no concern, but global radius of curvature (GRoC) is of concern and has a significant impact on telescope performance. The boundary condition segments can be thought of as four non-collinear points in three-dimensional space. The four non-collinear points define a reference sphere. If any or all of the coordinates of the four points change in 3-dimensional space, the motion changes the shape and orientation of the sphere the four points define.

The control system in equations 1.4 and 1.5 was derived to minimize the global variance of the edge shear errors subject to the constraint that the four prescribed segments do not move in their piston degrees-of-freedom. This way the control system maintains edge continuity on the reference sphere while the four boundary condition segments stay fixed. However, one cannot expect that the boundary condition segments do not move in piston. Boundary condition piston motion drives the control system to match up segment edges to fit a different sphere than the reference sphere. In fact, since the control system corrects all other modes of the primary mirror, the only way the primary mirror's sphere can change is by the control system changing its shape subject to motion of the boundary condition segments. A unique way of dealing with the control system interaction with boundary condition motion has been developed and verified[3]. The next sections of this paper describe how the edge-matching control system is integrated with GRoC maintenance.

2. CONTROL SYSTEM FUNCTIONAL DESCRIPTION

The SAMS optimal control system is implemented in software in "Operate" mode[3]. Operate mode is the normal mode during which the SAMS computer acquires sensor measurements from the Stackable System Processor (SSP)

and computes tip, tilt and piston commands to give to the PMC (Primary Mirror Computer). Figure 2 is a block diagram illustrating the flow of Operate mode.

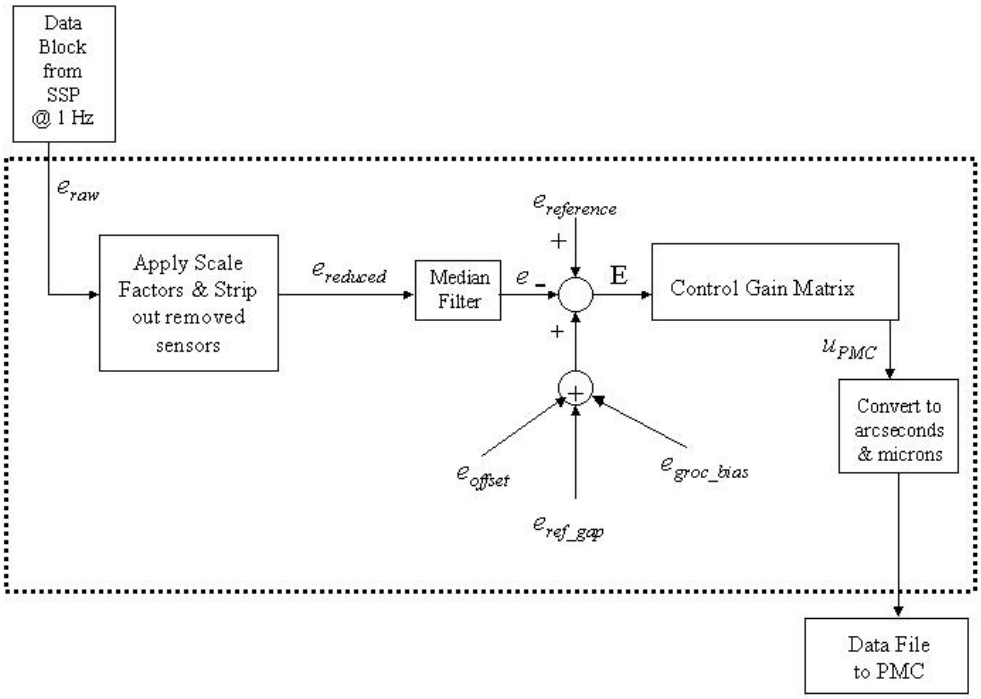

Figure 2: Operate mode flow diagram

The SAMS computer obtains edge sensor data from the SSP. The SSP provides the vector e_{raw}, a 546x1 vector. The vector contains six signals from every mirror segment, even from segments (especially the outer ring segments) that don't have a full complement of six edge sensors. After e_{raw} is read in, a scale factor is applied to the entire vector in order to convert the numbers to engineering units. The full range of valid edge sensor values is +/- 384 microns. After the scale factor is applied, the numerical values corresponding to sensors not present in the array are stripped out. Edge sensors that are not present include the locations on the outer ring, where there is no target sensor head, and any other internal locations where sensors, for whatever reason, have been removed from SAMS. Under nominal conditions the 546x1 vector e_{raw} is converted to a new 480x1 vector named $e_{reduced}$.

After applying scale factors and stripping out absent edge sensors, the remaining measurements are filtered. The SAMS console queries the SSP once every second to sample the edge sensor data. Ten consecutive samples are taken and then processed in a boxcar median filter. Originally a 10-sample average was calculated, but that filter had difficulties in rejecting invalid sensor values. The median filter has an effect similar to averaging, but it remains insensitive to random data glitches while catching sensor values that have hit saturation and stay there. The vector e, the output of the median filter, is generated approximately once every 10 seconds.

After the signals emerge from the median filter, the SAMS error signals are ready for conversion to tip, tilt and piston commands to mirror segments. The total SAMS edge sensor error signal, E, is defined by the following equation:

$$E = e_{reference} - e + e_{offset} + e_{ref\_gap} + e_{groc\_bias} \qquad (2.1)$$

The vector $e_{reference}$ contains all edge sensor values that were sampled when the current reference was set upon aligning the 91 mirrors to best image quality. The vector e_{offset} contains the edge sensor offset values prescribed by the telescope operator (TO). For example, if the TO desires to steer out a single mirror to evaluate the single-mirror seeing, the TO can command that motion through e_{offset}. The vector e_{ref_gap} contains the offset values prescribed by the gap-based GRoC compensator. Vector e_{ref_gap} has nonzero values only in the places held by sensors that directly sense M43 motions. Vector e_{groc_bias} comes from the GRoC estimator and has nonzero values only in places held by sensors directly sensing the boundary conditions (M43, M74, M25 and M28).

The next step is the generation of the control command for the mirror segments. The control command is generated from the following matrix equation:

$$u_{PMC} = KE \tag{2.2}$$

The output, u_{PMC} is a 273x1 vector which includes all the tip, tilt and piston corrections. Zeros are padded into u_{PMC} at the locations occupied by the boundary condition degrees of freedom. Segment tips and tilts are in units of radians, and pistons are in units of meters. After u_{PMC} is computed, the tip and tilt values are converted to arcseconds, and the piston values are converted to microns. After the unit conversion, all 273 values are written out to a file in the format prescribed by the SAMS Interface Control Document. Each set of tip, tilt and piston commands is accompanied by a sequence number which is assigned by the SAMS server software. That sequence number is referenced later when using the executed commands in the GRoC estimator.

The following subsections describe the origin of the control system reference parameters e_{ref_gap} and e_{groc_bias}. These two bias parameters deal with two separate GRoC-related phenomena associated with the HET and SAMS. The set point modifications specified in e_{ref_gap} deal with the change in radius-of-curvature of the mirror support structure, while the biases in e_{groc_bias} take care of the GRoC mode changes caused by control system interaction with boundary condition motion.

Section 2.1: The Phenomenon of truss-deformation-based GRoC change

The gap-based GRoC compensation scheme is based upon the hypothesis that the stainless steel truss behaves, in the mean, like a linear, elastic structure. It also is assumed that the truss sits on the telescope structure on an approximately kinematic mount. These assumptions allow one to conceive of the truss as a homogeneous bowl. The outer bowl in Figure 3 shows a mirror segment mounted on the bowl (truss) with its nominal radius of curvature. In this nominal position, the segment's center of curvature coincides with the center of curvature of the entire primary mirror. This condition reflects a perfectly aligned primary mirror. If a constant temperature change is applied at all points on the bowl (truss), the bowl will change shape. If the temperature change warms the truss, the bowl will expand, causing the bowl's RoC to grow. If the temperature change cools the truss, the bowl will contract, causing the

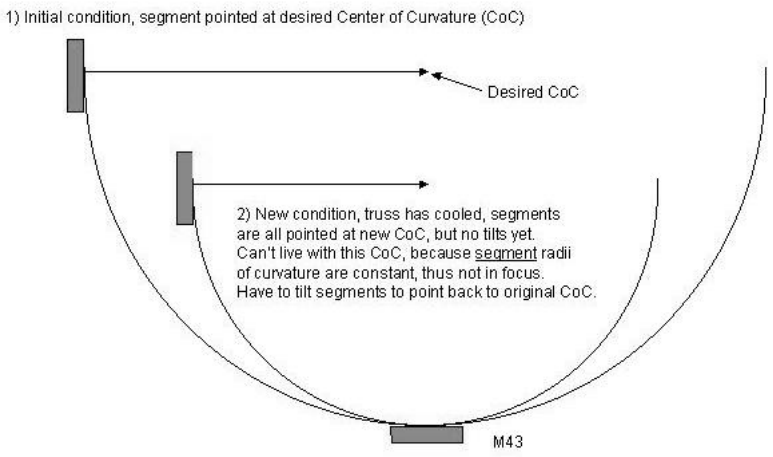

Figure 3: Change in sphere after temperature cools

bowl's RoC to shrink. The inner bowl in Figure 3 shows the bowl and segment positions after a uniform temperature drop.

After the truss has cooled, the bowl's radius of curvature has become smaller, but the individual mirror RoC's have remained the same. Thus the chief rays of each segment intersect at the bowl's new RoC, but the individual segments are out of focus. Thus the stacked image will be out of focus. Note that individual segments do not, themselves, move with respect to the bowl. That is, individual mirrors do not move in tip, tilt or piston during this physical phenomenon. They merely ride along the bowl that is changing shape.

One observes from Figure 3 that as the segments ride along the bowl, the size of the gaps between segments change. As the bowl cools, the gaps get smaller. As the bowl heats up, the gaps get larger. Preliminary testing [5] performed on the Hobby-Eberly Telescope from January-March 2000 indicated that the gap dimension changed at a rate of approximately 11.5 microns per degree C. That magnitude agrees with the dimensional change of a one-meter-long piece of stainless steel. During the Sub-array Test (SAT), the gap sensing capability of the edge sensors was exploited to measure the mean gap change among the SAT segments[6]. The SAT results indicated a mean gap change of 10.9 microns per degree C. These data supported the assumption of an, in the mean, linear elastic truss, kinematically mounted and undergoing a thermal soak. Furthermore, analysis indicated that gap changes of 11.5 microns per degree C correspond to global RoC changes of 300 microns per degree C.

One way of ameliorating the situation in Figure 3 is to steer the mirror segments to point their chief rays all at the original, nominal radius-of-curvature, thereby restoring all mirrors to their original positions on the original bowl. Figure 4 shows the applied correction. According to Figure 4, tip, tilt and piston commands to the mirrors can correct for GRoC changes caused by thermal expansion and contraction of the truss. Since the primary mirror array's mean gap change has been shown to be well correlated linearly with temperature change[6], and the gap measurements are obtainable from the gap sensing capability of the edge sensors, adequate information is available to generate a GRoC correction command. The next subsection shows how the GRoC correction command is generated from the change in mean gap and how the scheme is implemented in the SAMS control system.

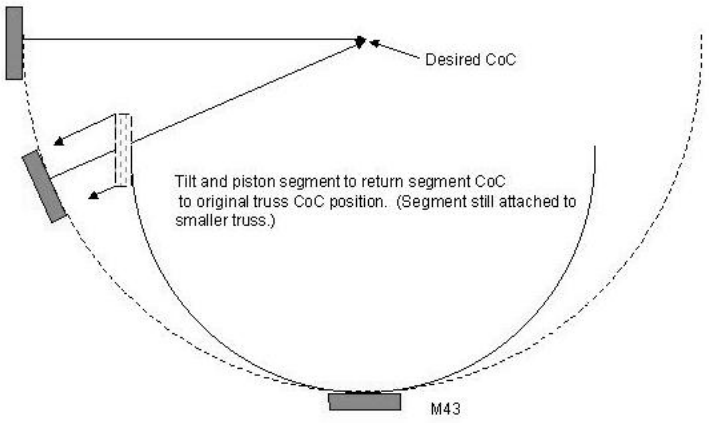

Figure 4: Mirror segment motions to correct GRoC

Section 2.2: Implementation of the gap-based GRoC control

The gap-based compensation is not a typical feedback control system. Rather it is an open-loop, feed-forward type of control. The sensed parameter is the change in mean gap size. SAMS and PMC have no way of controlling what the gap size is because there is no control over the segment lateral translational or clocking degrees of freedom. Rather, SAMS uses the change in mean gap to calculate what the mirror tip, tilt and piston positions should be in order to keep the segments pointed at the nominal radius of curvature.

The gap-based feed-forward compensation commands a GRoC mode to the SAMS. SAMS can induce a GRoC mode by pistoning the central boundary condition segment M43. The SAMS edge-matching control system then

tries to keep the edges matched up, but as M43 pistons up, SAMS will flatten out the bowl. As M43 pistons downward, SAMS will contract the bowl.

Since one cannot count on HET's actuator/mount/mirror assembly to be a "go-to" actuation system, open-loop pistoning M43 is not an accurate way of adjusting the GRoC. A more accurate approach is to command biases to the edge sensors which sense M43's motion such that the SAMS control system is tricked into thinking that M43 has moved in piston. This way, the control system will respond by either flattening out or folding up the segments adjacent to M43. The control system will make the rest of the array follow the inner ring segments in order to keep the edges matched up. Figure 5 shows the flow of the gap-based GRoC compensation loop.

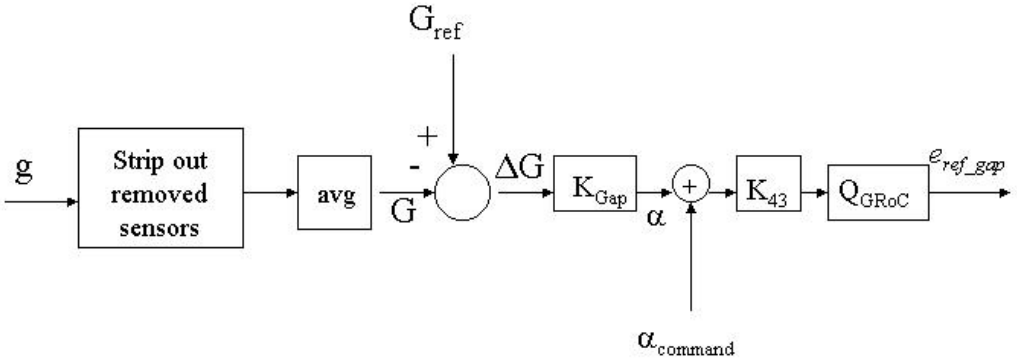

Figure 5: Gap-based GRoC compensation loop flow

The input to the gap-based GRoC compensator is g, a 546x1 vector of gap measurements taken at each edge sensor position. Like the 546x1 vector of raw edge sensor measurements, the vector g has the same structure as e_{raw}. That is, g includes places for 6 sensors per segment, whether or not a sensor head is actually mounted at a particular spot. The gap readings are not sampled as frequently as the shear readings. The gap measurements are sampled about once every 10 seconds. Blue Line Engineering, the edge sensor developer, asserts that the accuracy of the gap measurement is on the order-of-magnitude of 100 nanometers.

Just like in the Operate mode loop, the unused edge sensor locations are stripped out of vector g. Next, the mean of all active gap sensors is evaluated and assigned to scalar variable G. The change in mean gap, ΔG, is computed by subtracting the current mean gap, G, from the reference gap, G_{ref} . G_{ref} is defined as the mean gap at the time the current reference was set when the primary mirror was aligned. The change in mean gap is then scaled to an equivalent dihedral angle, α. The scale factor K_{Gap} converts the change in mean gap to an equivalent dihedral angle. The magnitude of K_{Gap} is –0.03794 radians/meter. The equivalent dihedral angle, α, is combined with a user-specified dihedral angle, $\alpha_{command}$. The user-specified dihedral angle enables the telescope operator to manually "joystick" the GRoC to any desired magnitude.

The next scale factor, K_{43} , converts the commanded dihedral angle to the equivalent piston magnitude required by M43 to achieve the prescribed change in GRoC. The magnitude of K_{43} is 4.5 meters of M43 piston per radian of dihedral angle. Once the equivalent M43 piston is computed, it is multiplied by the vector Q_{GRoC} . Q_{GRoC} is a 480x1 vector which is simply the column of the full-array influence matrix which relates edge sensor outputs of all 480 edge sensors to piston motion of M43. The result is vector e_{ref_gap}, a 480x1 vector of biases to the edge sensors. These are the biases that will cause the primary mirror to either contract or flatten out, depending on the truss temperature change and subsequent mean gap change. Vector e_{ref_gap} is then added into the error signal as shown in Figure 1.

Section 2.3: Implementation of GRoC estimator in SAMS

The Operate mode flow diagram in Figure 1 identified the vector e_{groc_bias}. The vector e_{groc_bias} is the output of the Global Radius of Curvature (GRoC) estimator. A detailed derivation of the GRoC estimator and its integration with the SAMS control system is located elsewhere in the literature[3]. In this paper, what follows is a description of how the GRoC estimator was interfaced with the SAMS control system while not interfering with the workings of the gap-based GRoC correction loop.

In the previous section, it was shown that the SAMS control system deliberately imparts a GRoC mode into the primary mirror in order to counteract the radius-of-curvature change caused by the thermoelastic deformation of the primary mirror support structure. Since the GRoC estimator's responsibility is to sense and correct any GRoC-mode motions the control system puts into the primary mirror, the GRoC estimator will try to undo the gap-based GRoC adjustments made by the control system. The GRoC estimator loop must be made smart enough to know not to undo gap-based GRoC corrections. Figure 6 shows how the GRoC estimator is implemented while benignly coexisting with the gap-based GRoC compensator.

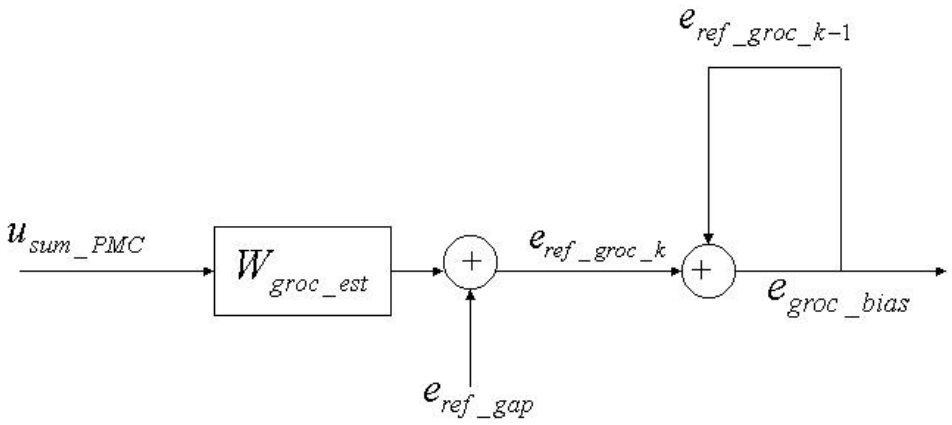

Figure 6: GRoC estimator flow diagram

The block diagram of Figure 6 is summarized by equations 2.3 and 2.4:

$$e_{groc\_bias} = W_{groc\_est} u_{sum\_PMC} + e_{ref\_gap} + e_{ref\_groc\_k-1} \tag{2.3}$$

$$e_{ref\_groc\_k-1} = e_{groc\_bias} \tag{2.4}$$

The input to the GRoC estimator is u_{sum_PMC}, the sum of all tip, tilt and piston motion commands executed by the PMC since the current edge sensor reference was set. W_{groc_est} is the GRoC estimator matrix. The output vector $e_{ref\_groc\_k}$ is an intermediate edge sensor bias value which corresponds to the change in GRoC since the last data interval k-1. The vector e_{groc_bias} is the edge sensor bias that is added to the edge sensor error signal in the edge sensor control loop. After the bias is updated, the bias at interval k is assigned to $e_{ref\_groc\_k-1}$ for the next cycle of the loop. Finally, the GRoC estimator edge sensor biases are accumulated so that the current bias is held and added upon as more perturbations affect the boundary conditions.

The edge sensor bias from the mean-gap-based GRoC compensator, e_{ref_gap} , is added in the GRoC estimator loop so that the GRoC estimator doesn't undo whatever gap-based GRoC corrections were previously put in. It is added rather than subtracted because inherent to W_{groc_est} is a negative sign. Since the estimator, by itself, estimates the state, the state must be negated for a correction to apply.

3. SAMS PERFORMANCE ON THE HOBBY-EBERLY TELESCOPE

Full-array SAMS hardware installation was completed by September 2001. The full-array SAMS software (minus the GRoC estimator) was installed and verified in October 2001. The full-array SAMS became operational for nighttime astronomical use in October 2001. A final software installation, which included the GRoC estimator, was completed in December 2001. Verification of software functionality was completed in December 2001. Through May 2002, engineering data were compiled in order to characterize the overall performance of the HET with SAMS. Evaluation of SAMS over such an extended time interval allowed the observation of SAMS subject to the changes of seasons and the temperature extremes that accompany them. During that time interval SAMS was subjected to an operational temperature range from –10 degrees C to +25 degrees C. Performance characterization data indicated that SAMS maintains the primary figure very well when subject exclusively to low-frequency segment-motion dynamics, but SAMS does not maintain the figure well when the temperature changes more than 1.5 degrees C from the reference temperature.

A good illustration of SAMS's ability to maintain the primary mirror figure in the presence of low-frequency dynamics is the examination of closed-loop versus open-loop edge sensor time histories. Figure 7 shows the time histories of edge sensors on a single segment, M27, on the night of November 26, 2001. In the time interval shown, during the first two-and-a-half hours, the telescope operator was using SAMS with HET to perform astronomical observations. Over the last one-and-a-half hours, the SAMS/PMC loop was opened. During that time, edge sensor data was acquired, but no mirror corrections were applied. Figure 7 shows that when the loop is opened, mirror motion dynamics cause the edge sensors to sense report motions on the order of 1 micron per hour. When the loop is closed, edge sensor shear readings stay within about 100 nanometers RMS.

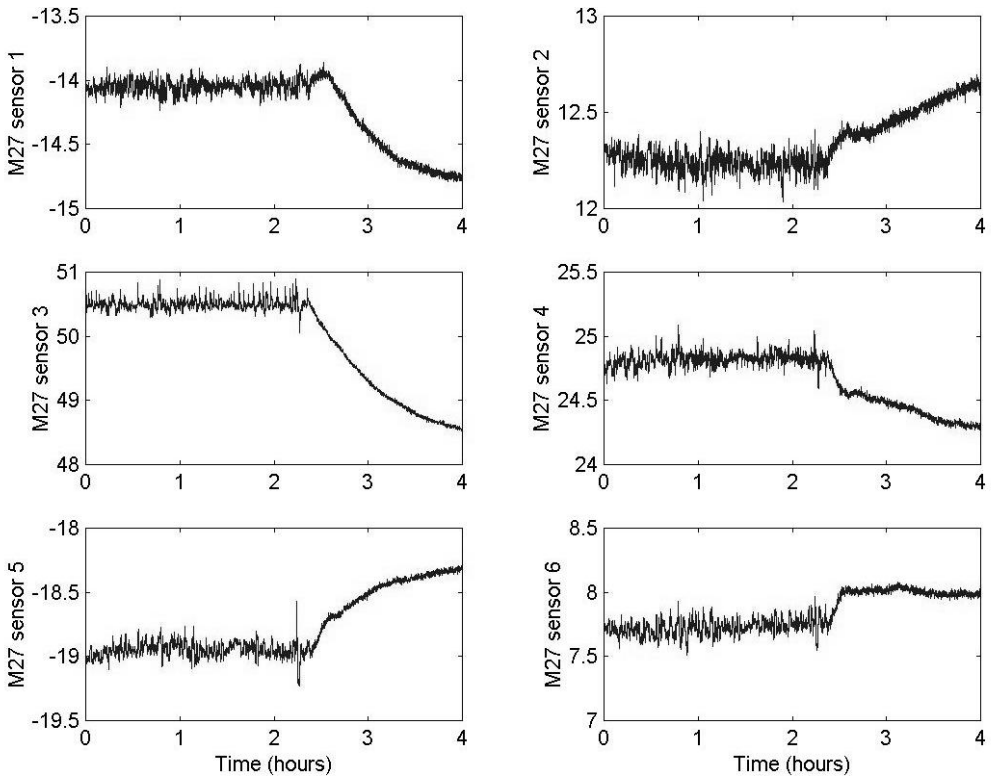

Figure 7: M27's Edge Sensors (microns) 11/26/2001 02:51-06:51 CST

The time histories in Figure 7 were acquired during a period when the temperature changed very little. The telescope operators have observed gradual image degradation as temperature changes throughout the night. From April 1, 2002 through May 31, 2002, image quality data were recorded along with temperature change data. The image degradation (50% encircled energy) versus temperature change was quantified in the plot in Figure 8. Figure 8 comprises 70 data points compiled over the two-month period. A parabolic curve was fit to the data. Equation 3.1 quantifies the best curve fit.

$$\Delta EE50 = 0.1159(\Delta Temp)^2 \qquad (3.1)$$

Within a temperature range of +/- 0.5 degrees C about the reference temperature, the image degradation stays within 0.16 arcseconds. The telescope operator's EE50 measurement accuracy is about 0.1 arcseconds. Figures 7 and 8 together show that when the disturbance environment is dominated by low-frequency dynamics, SAMS maintains the primary mirror figure and resultant image quality within the noise limitations of the edge sensor system.

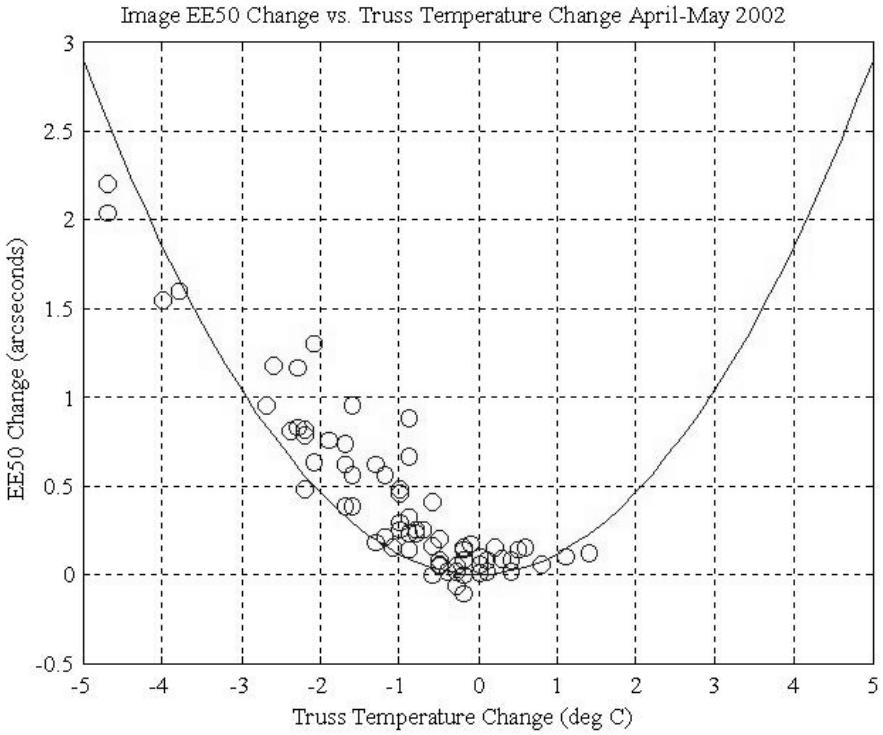

Figure 8: Image Degradation vs. Temperature Change (April-May 2002)

Beyond +/- 0.5 degrees of the reference temperature, Figure 8 indicates that HET's image quality suffers as temperature changes. When the truss temperature has changed 1.5-2.0 degrees C, the image quality has degraded about 0.5 arcseconds or more. At that point, image quality is unacceptable for astronomical observations, and the telescope operator must realign the primary mirror and set a new SAMS reference.

How often must the telescope operator realign the primary mirror? In order to assess, on average, how frequently the mirror must be realigned in order to accomodate current SAMS performance limitations, peak-to-peak nighttime truss temperatures were compiled over the first four-month period during which SAMS was operational. The plot in Figure 9 shows the percentage of nights in which the temperature changed specific amounts. Data points excluded

from this plot included nights when significant weather events (rain, snow, ice, fog, humidity or dust) required dome closure. The steep temperature changes that accompanied such nights would not have affected the realignment frequency since no science was performed on those nights. Assuming that on average the telescope operator must realign the mirrors at every 1.5-degree C temperature change, 20 percent of all nights require no additional realignments after the initial stack upon dome opening. 70 percent of all nights (3-degree C or less temperature change) require one additional restack, and 90 percent of all nights (4.5-degree C or less temperature change) require up to two additional restacks. Examination of HET night reports reveals that on most nominal science nights, two additional restacks are required. A night which involves three additional restacks is a 3-sigma event.

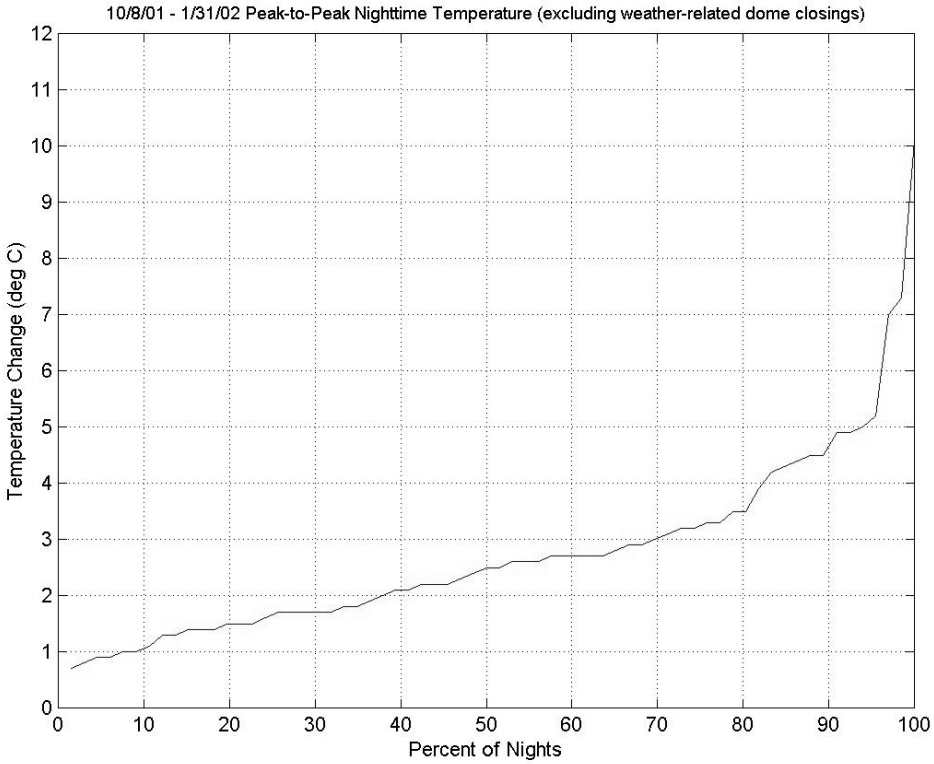

Figure 9: HET Truss Temperature Change vs. Percentage of Nights

The dominant contributor to image degradation with SAMS is temperature-dependent drift in the inductive edge sensors. Inductive edge sensors are known to be sensitive to temperature change. At the Sub-array Test, temperature-dependent edge sensor drift was observed, and its effects on the control system metric J were quantified[2]. Temperature-dependent drift effects on the control system metric were also quantified for the full-array SAMS[7]. Temperature changes can affect the output of inductive edge sensors by altering both the sensor scale factor (also known as gain) and bias (or zero offset). Since every sensor has two parameters to ascertain, calibration of 960 parameters was required.

Early in the SAMS project Blue Line Engineering conceived a strategy to calibrate both scale factor and bias. Scale factor calibration involved pistoning each segment through a prescribed range in discrete steps while recording the edge sensor readings at each step. This procedure would produce edge sensor output versus piston motion curves. The slope of the curve would be the scale factor at that particular temperature. The procedure would then be repeated at several different temperatures, and new curves obtained by plotting scale factor versus temperature. Calibration of the biases intended to exploit edge sensor measurments recorded when the telescope operator stacked the array at different temperatures. The recorded edge sensor measurments would be compensated by the scale

factors derived from the scale factor calibrations. Assuming that the stacked array represented the uniquely best image quality, any residuals in the edge sensor measurements would be attributed to biases.

Inherent limitations in HET systems and operations impeded successful implementation of the two calibration schemes. The scale factor calibration was hindered by the HET's actuator/mount/mirror assembly not being a high enough fidelity and repeatable positioning system. Actual piston motions varied from 60-130 percent of commanded motion and were not repeatable. Piston motions also coupled into significant tip and tilt motions. Without a sufficiently accurate fiducial sensor to measure the true position of the mirror, the scale factor calibration tests yielded noisy data dominated by the mirror motion uncertainties. The bias calibration scheme was further complicated by the inherent errors involved in the mirror stacking process. Field testing revealed that the stacking process has an inherent global tilt caused by small misalignment of the primary mirror's boresight with the alignment tower. Since stacking is performed with tip and tilt motions only (no piston), stacking induces a stairstep, or "Venetian blind," mode into the primary mirror. Boresight misalignments of fractions of an arcsecond yield edge sensor output changes on the order of 10 microns at the stairsteps. Since the edge sensor drift is on the order of 10 - 100 nanometers per degree C, the stairstep mode drowns out any signal from temperature-dependent biases or scale factors.

Application of estimation techniques to closed-loop edge sensor time histories were investigated. Estimating 960 parameters from a primary mirror which can deform in only 273 unique degrees of freedom or mode shapes was a highly underdetermined problem. Even if one attributed all drift in each edge sensor channel to a single parameter, there still remained a problem of 480 parameters with only 273 unique degrees of freedom, still a highly underdetermined problem. At this time there exists no closed-form solution of the edge sensor temperature drift parameter estimation problem. Nor does there exist adequate metrology against which to calibrate the edge sensors *in situ* on the telescope. Until a satisfactory calibration scheme can be conceived, proven by analysis and test, and implemented, SAMS will continue to be sensitive to temperature-dependent drift in the edge sensors. Nighttime operations of HET will continue to require up to two or three restacks per night, depending on the magnitude of temperature change.

REFERENCES

1. J. Booth, M. Adams, G. Ames, J. Fowler, E. Montgomery, J. Rakoczy, "Development of the Segment Alignment Maintenance System (SAMS) for the Hobby-Eberly Telescope," *Optical Design, Materials, Fabrication, and Maintenance*, SPIE **4003**, No. 20, Munich, Germany, March 27-31, 2000.
2. J. Rakoczy, D. Hall, R. Howard, J. Weir, E. Montgomery, G. Ames, T. Danielson, P. Zercher, "Demonstration of a Segment Alignment Maintenance System on a seven-segment sub-array of the Hobby-Eberly Telescope," *Adaptive Optics Systems and Technology II*, SPIE **4494**, pp. 69-80, San Diego, California, July 30 – August 1, 2001.
3. J. Rakoczy, D. Hall, W. Ly, R. Howard, E. Montgomery, "Global radius-of-curvature estimation and control for the Hobby-Eberly Telescope," *Large Ground-Based Telescpes*, SPIE **4837**, No. 79, Waikoloa, Hawaii, August 21-28, 2002.
4. D. Hall, W. Ly, R. Howard, J. Weir, J. Rakoczy, "Software development for the Hobby-Eberly Telescope's Segment Alignment Maintenance System using LabVIEW," *Advanced Telescope & Instrumentation Control Software II*, SPIE **4848**, No. 25, Waikoloa, Hawaii, August 21-28, 2002.
5. J. Lindner, T. Driskill, "Hobby-Eberly Telescope Gap Characterization Data Package," NASA Internal memo No. ED27-01-114, October 18, 2001.
6. J. Rakoczy, "Sub Array Test Review," Segment Alignment Maintenance System Critical Design Review Data Package, May 1, 2001.
7. J. Rakoczy, "Segment Alignment Maintenance System Performance on the Hobby-Eberly Telescope," NASA Internal memo No. SD71-006-02, February 14, 2002.
8. J. Rakoczy, "Hobby-Eberly Telescope Segment Alignment Maintenance System Control System Equations Document," NASA Internal memo No. SD71-007-02, February 21, 2002.